



## Quench Margin at Injection

W. Bartmann, C. Bracco, B. Goddard, B. Holzer, M. Bednarek, E. Nebot Del Busto, A. Nordt, A. Priebe, S. Redaelli, M. Sapinski, R. Schmidt, M. Solfaroli, A. Verweij, M. Zerlauth.

Keywords: Quench margin and BLM calibration

---

### Summary

The results of the MD performed on July the 3<sup>rd</sup> to address the quench margin at injection for Q6.L8 and Q4.L6 magnets are presented in this note.

---

### 1. Introduction

On April 18<sup>th</sup>, as a consequence of a flash over at the MKI D, 36 bunches of Beam 2 were kicked with 75-90% of the nominal kicker deflection. Nearly all the protons of these bunches impacted on the TDI and TCLIB jaws inducing the quench of 11 downstream magnets. As a follow-up of this event, the angular alignment of the TDI was rechecked [1] and the aperture of the TCLIB was relaxed by  $1.5 \sigma$ , in order to minimize the number of primary protons intercepted at this collimator and the load on the downstream magnets (in particular Q6.L8).

A dedicated MD has been carried out, on July 3<sup>rd</sup>, to quantify the loss rate at the Q6.L8, as a function of different TCLIB settings, and to define the quench margin of this magnet at injection. Special QPS monitoring systems and one permanent filtered BLM [2] have been installed on the selected magnet and next to the TCLIB. A similar measurement has also been performed to define the quench margin at the Q4.L6 downstream of the B2 TCDQ and for BLM calibration.

### 2. Quench margin for Q6.L8 during Beam 2 injection

Two methods were employed to measure the quench limit of Q6.L8 at injection and are described in the following. Pilot bunches with different intensities were injected and two primary collimators in IR7 (TCP.C6R7.B2 and TCP.D6R7.B2) were closed to 1 mm gap and - 2 mm offset in order to stop the beam and trigger a beam dump with "post mortem" data. Collimator position thresholds were opened to parking and interlocks were masked to allow injection with these special collimator settings.

## 2.1 First method: injection with different TCLIB settings

The first method consisted in injecting a pilot bunch with different TCLIB settings and monitoring the losses at the collimator and downstream magnets (Q6 and Q7), and the QPS signal at the Q6.L8. Few reference shots were taken with the TCLIB at  $8.3 \sigma$ ; the jaws were then closed in steps of  $2 \sigma$  until a half-gap of  $2.3 \sigma$  and of  $0.5 \sigma$  until  $1.3 \sigma$ . This last aperture corresponds to a gap of  $\sim 1$  mm, very close to the anti-collision limit. In order to intercept the full beam, an offset of up to  $3 \sigma$ , with respect to the beam centre, was applied while keeping the minimum gap.

The measurement was repeated with increasing bunch intensity:  $1 \times 10^{10}$ ,  $2 \times 10^{10}$  and  $3 \times 10^{10}$  protons. The emittance, measured in the SPS, varied from  $0.8 \mu\text{m}$  to  $1 \mu\text{m}$  in the horizontal plane and staid constantly at  $1 \mu\text{m}$  in the vertical plane, for the different intensities.

The signal from the BLM presented in Table 1 (see Fig. 1 for schematic layout) was analyzed:

**Table 1**

Name and dcum of BLM used for data analysis

Beam 1		Beam 2	
Expert Name	dcum	Expert Name	dcum
BLMQI.06L8.B1E30_MQML	23093.130	BLMEI.06L8.B2I10_TCLIB.6L8.B2	23096.860
BLMQI.06L8.B1E20_MQML	23086.240	BLMES.06L8.B2I10_TCLIB.6L8.B2	23096.860
BLMQI.06L8.B1E10_MQML	23080.810	BLMEI.06L8.B2I11_TCLIB.6L8.B2	23096.860
BLMQI.07L8.B1E30_MQM	23069.530	BLMQI.06L8.B2I10_MQML	23088.510
BLMQI.07L8.B1E20_MQM	23062.450	BLMQI.06L8.B2I20_MQML	23085.240
BLMQI.07L8.B1E10_MQM	23059.110	BLMQI.06L8.B2I30_MQML	23077.360
		BLMQI.07L8.B2I10_MQM	23065.980
		BLMQI.07L8.B2I20_MQM	23061.450
		BLMQI.07L8.B2I30_MQM	23055.900

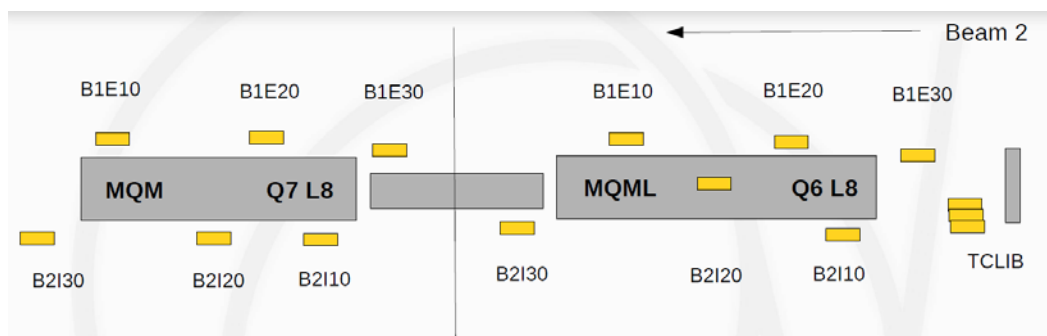


**Figure 1**

Schematic view of the position of the BLMs at the location of the MQ magnets downstream of the TCLIB

The summary of the events, sorted by time, is presented in Table 2.

**Table 2**

Events sorted by TCLIB aperture. The local time refers to July 3<sup>rd</sup> 2011.

Shot Number	Time (local)	Intensity [ $\times 10^{10} \text{ p}^+$ ]	TCLIB half-gap [ $\sigma$ ]
1	15:21:49	1	8.3 (reference)
2	15:31:11	1	8.3 (reference)
3	17:18:28	1	6.3
4	17:28:32	1	6.3
5	17:33:35	1	4.3
6	17:38:37	1	4.3
7	17:43:40	1	2.3
8	17:48:42	1	2.3
9	17:54:28	1	1.8
10	17:58:47	1	1.8
11	18:03:06	1	1.3
12	18:08:52	1	1.3
13	18:16:04	1	1.3 + 1 $\sigma$ offset
14	18:21:49	1	1.3 + 1 $\sigma$ offset
15	18:25:25	1	1.3 + 2 $\sigma$ offset
16	18:30:28	1	1.3 + 2 $\sigma$ offset
17	18:52:04	2	8.3 (reference)
18	18:57:06	2	6.3
19	19:03:35	2	4.3
20	19:10:04	2	2.3
21	19:14:23	2	2.3
22	19:18:42	2	1.8
23	19:26:37	2	1.8
24	19:30:13	2	1.3
25	19:33:49	2	1.3
26	19:38:52	2	1.3 + 1 $\sigma$ offset
27	19:42:28	2	1.3 + 1 $\sigma$ offset
28	19:46:47	2	1.3 + 2 $\sigma$ offset
29	19:50:23	2	1.3 + 2 $\sigma$ offset
30	19:53:59	2	1.3 + 2 $\sigma$ offset
31	20:11:16	3	1.3 + 2 $\sigma$ offset
32	20:16:18	3	1.3 + 2 $\sigma$ offset
33	20:21:20	3	1.3 + 2 $\sigma$ offset
34	20:25:40	3	1.3 + 2 $\sigma$ offset
35	20:32:08	3	1.3 + 3 $\sigma$ offset

### 2.1.1 BLM analysis

Losses at Q6.L8 and Q7.L7 were analyzed, for the different intensities, as a function of the TCLIB settings. Running sum 01 (corresponding to an integration time of 40  $\mu$ s) was considered in order to investigate only losses happening during the beam injection.

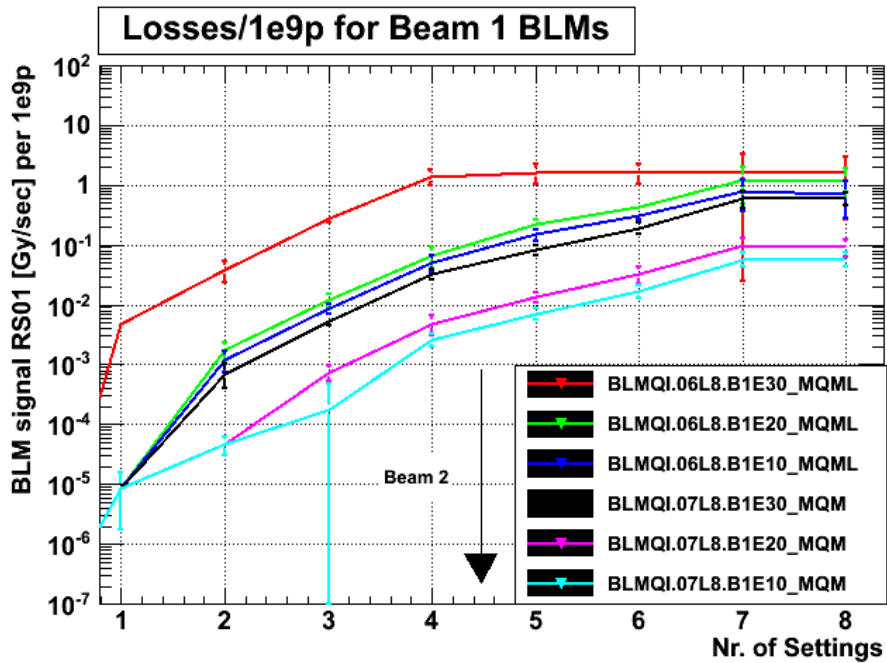


Figure 2

The average of the losses, normalized with respect to the beam intensity, recorded at the B1 MQ6 and MQ7, as a function of the TCLIB, setting is presented

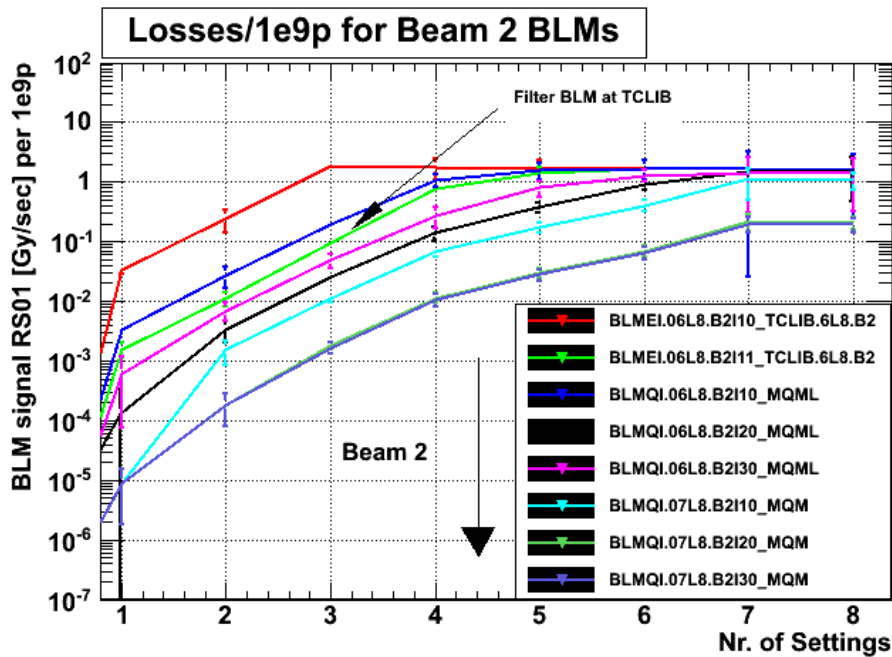


Figure 3

The average of the losses, normalized with respect to the beam intensity, recorded at the B2 TCLIB, MQ6 and MQ7, as a function of the TCLIB, setting is presented.

The monitors in position 3 for B1 and position 1 for B2 on Q6 (i.e. Q6L8 B1E30 and Q6L8 B2I10, see Fig. 1) were in saturation for all the shots with a TCLIB half-gap smaller than  $2.3 \sigma$ , while the BLMs on Q7 did not saturate. The average of the losses, normalized to the beam intensity, for the monitors on TCLIB, Q6L8 and Q7L7 was calculated, for each TCLIB setting, and is presented in Fig. 2 and Fig. 3.

Eight main settings were used: “setting 1” corresponds to  $8.3 \sigma$  and “setting 8” to a half-gap of  $1.3 \sigma$  with  $2 \sigma$  offset (see Table 2). The normalized losses increase for smaller apertures at the TCLIB while there is no significant difference between the settings with a half-gap of  $1.3 \sigma$  plus  $1 \sigma$  or  $2 \sigma$  offset. This is expected and indicates that the full beam was intercepted by the TCLIB. An additional ionization chamber (BLMEI.06L8.B2I11\_TCLIB.6L8.B2), with a RC delay ( $R=150k\Omega$ ,  $C=47nF$ ), was installed at this collimator in preparation of the MD. This was done in order to overcome the problem of saturation and to be able to correlate the BLM reading with the number of protons lost at the collimator. The signal from the two ionization chambers, with and without RC filter, and the SEM at the TCLIB was investigated for all the events listed in Table 2 and is shown in Fig. 4.

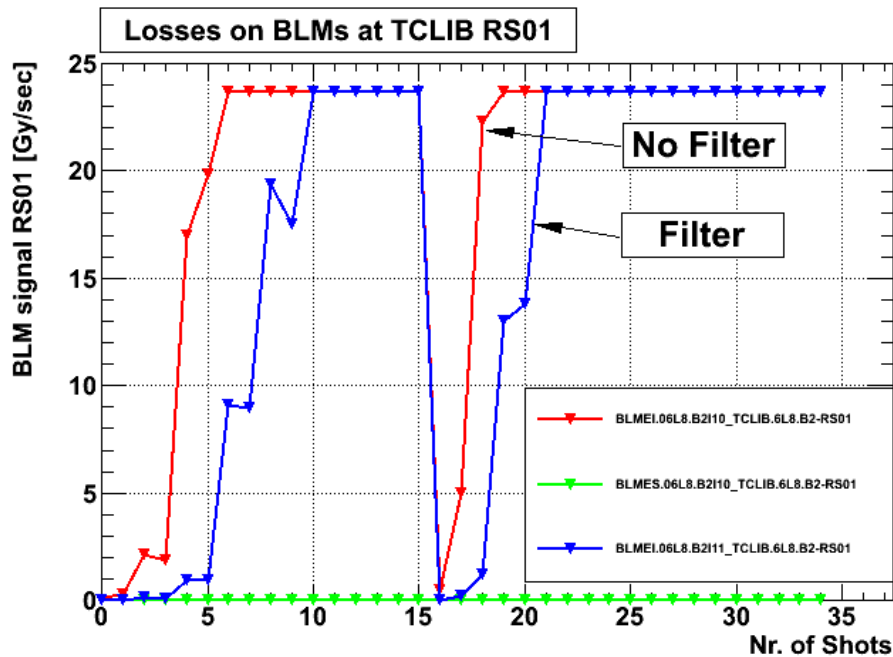


Figure 4

Signals of the ionization chambers, with and without RC filter, and the SEM installed at the TCLB for all the analyzed events.

The SEM did not record any signal while both BLMs reached saturation even if the filtered BLM was expected to show a signal a factor of 180 smaller than the ionization chamber without filter. In reality, the linear correlation between losses at the 'normal' and the filtered BLMs (see Fig. 5), when not in saturation, gave a reduction factor of  $18.64 \pm 0.72$ , that is one order of magnitude smaller than the theoretical one. It was then not possible to calibrate the TCLIB BLM but, to define the load on the downstream magnets, we assumed that the full injected intensity was impacting at the TCLIB when closed at  $1.3 \sigma + 2 \sigma$  offset. The load at the Q6.L8 has been calculated taking into account the BLM in the middle position, considering a calibration factor of  $4.57 \times 10^{-13} \text{Gy/p}^+$ .

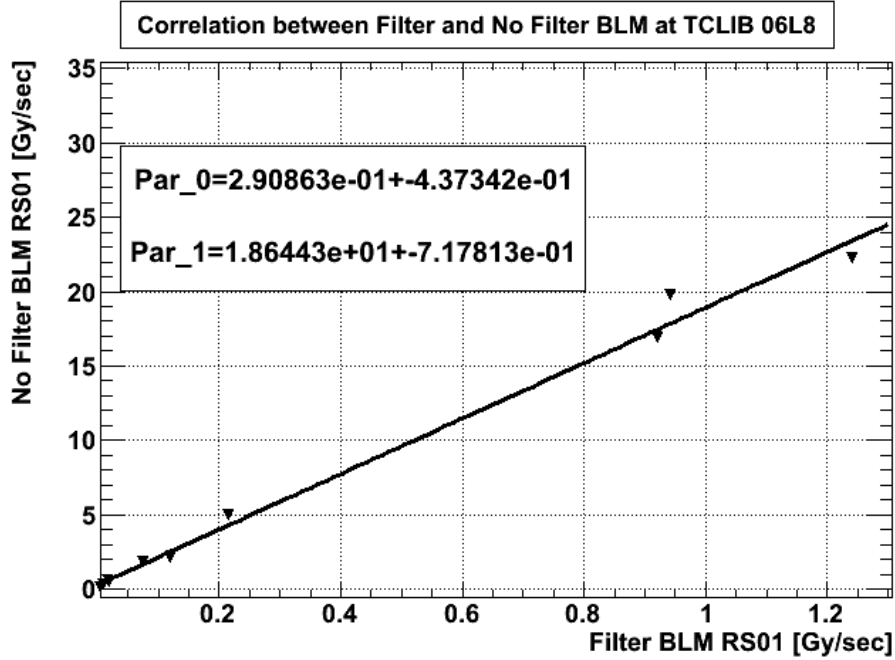


Figure 5

Linear correlation between filtered and not filtered TCLIB BLM signals.

The number  $n_p$  of protons lost at the magnet and corresponding to a certain loss level  $L$  [Gy/s] at the BLM can be defined as:

$$n_p = \frac{L \cdot T}{4.57 \times 10^{-13}} \quad (1)$$

where  $T$  is the integration time (40  $\mu$ s in this case).

The BLMQI.06L8.B2I20\_MQML did not saturate when injecting the full  $1 \times 10^{10} p^+$  bunch on the TCLIB (setting 8). A loss of 21.3 [Gy/s] was recorded corresponding to  $1.9 \times 10^9 p^+$  that is about 20% of the particles intercepted by the TCLIB. This monitor was in saturation for the same TCLIB setting and higher intensity; it has then been tried to estimate the loss at the Q6.L7 out of the ratio between B2 and B1 monitors.

The ratio between BLMQI.06L8.B2I20\_MQML and BLMQI.06L8.B1E10\_MQML stayed relatively constant to about 2.5 over the different TCLIB settings (see Fig. 6, values equal to 0 correspond either to B2I20 in saturation or lost data: shots 1-2). The B1 monitor has been used to reconstruct the losses at the B2 saturated monitor: B2 loss = B1 loss  $\times$  2.5. The number of protons lost at the Q6.L8 and the ratio with respect to the injected intensity could be calculated for each shot (see fig. 7). The load on the Q6.L8 magnet is estimated to be about 10 % -20 % of the beam impacting on the TCLIB (data corresponding to setting 8).

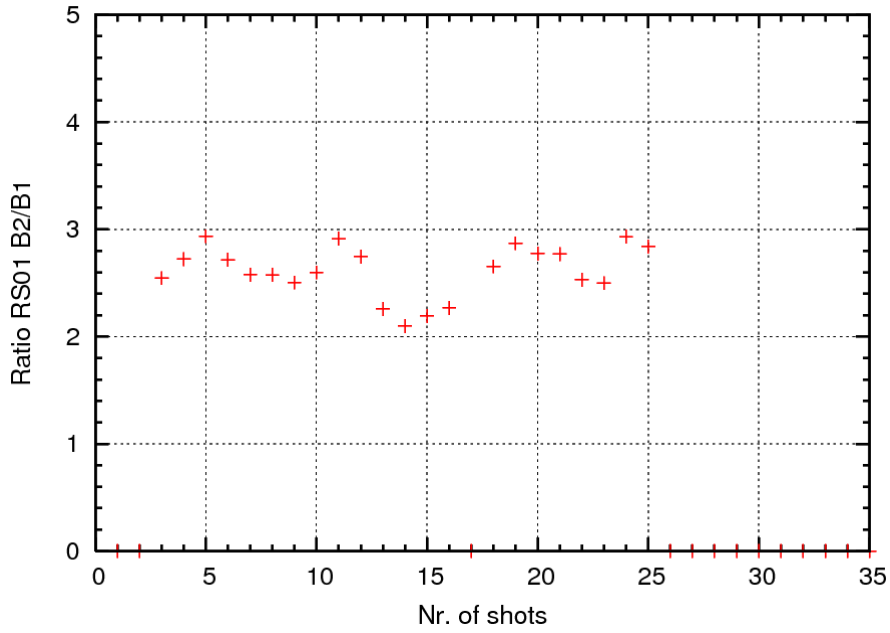


**Figure 6**

Ratio between BLMQI.06L8.B2I20\_MQML (B2) and BLMQI.06L8.B1E10\_MQML (B1) for the events presented in Table 2. Zero values correspond either to B2I20 saturation or lost data (shots 1-2).

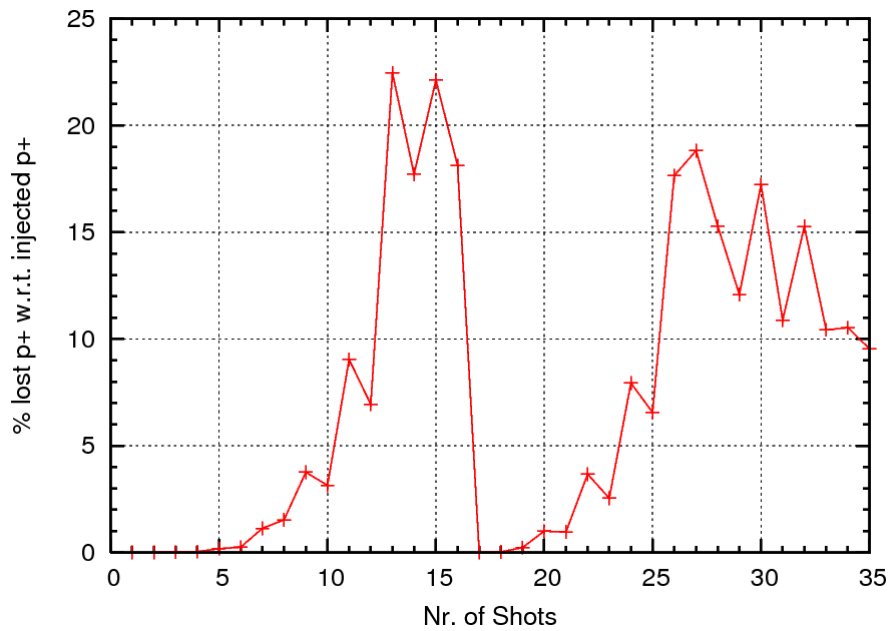


**Figure 7**

Percentage of protons lost at the Q6.L8 with respect to injected intensity, for all the events presented in Table 2. The signal of BLMQI.06L8.B2I20\_MQML, when saturated, was reconstructed starting from BLMQI.06L8.B1E10\_MQML signal (Loss B2 = Loss B1  $\times$  2.5).

### 2.1.2 QPS analysis

The electrical signal was picked up in parallel to the QPS system. A special patch was prepared so that the QPS system can work normally, assuring the standard level of protection. A digital voltmeter system was based on NI USB-6251 8-channel ADC. The final sampling rate was set to 10 kHz. A detailed system description can be found in [2].

On Q6.L8 many signals were acquired in correlation with the beam losses generated on TCLIB. These signals were observed only on B2 aperture coils, while on the B1 aperture no signal went out of the noise level.

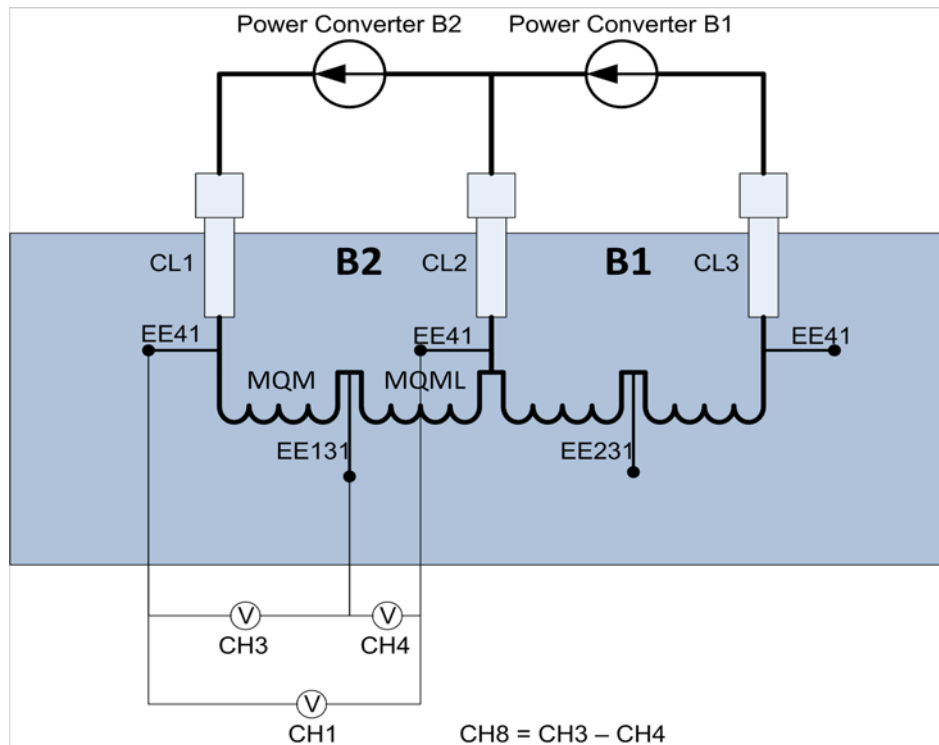


**Figure 8**

Electrical connections of B2 aperture. B1 wiring not shown - for simplicity.

The correctness of electrical connections (Fig. 8) was checked by recording a current ramp in the magnet (Fig. 9). Measurement channels recorded then  $L \frac{dI}{dt}$  and thanks to this the polarity and gain of each channel were verified (Fig. 10).





**Figure 9**  
Current ramp in Q6.L8 magnet.

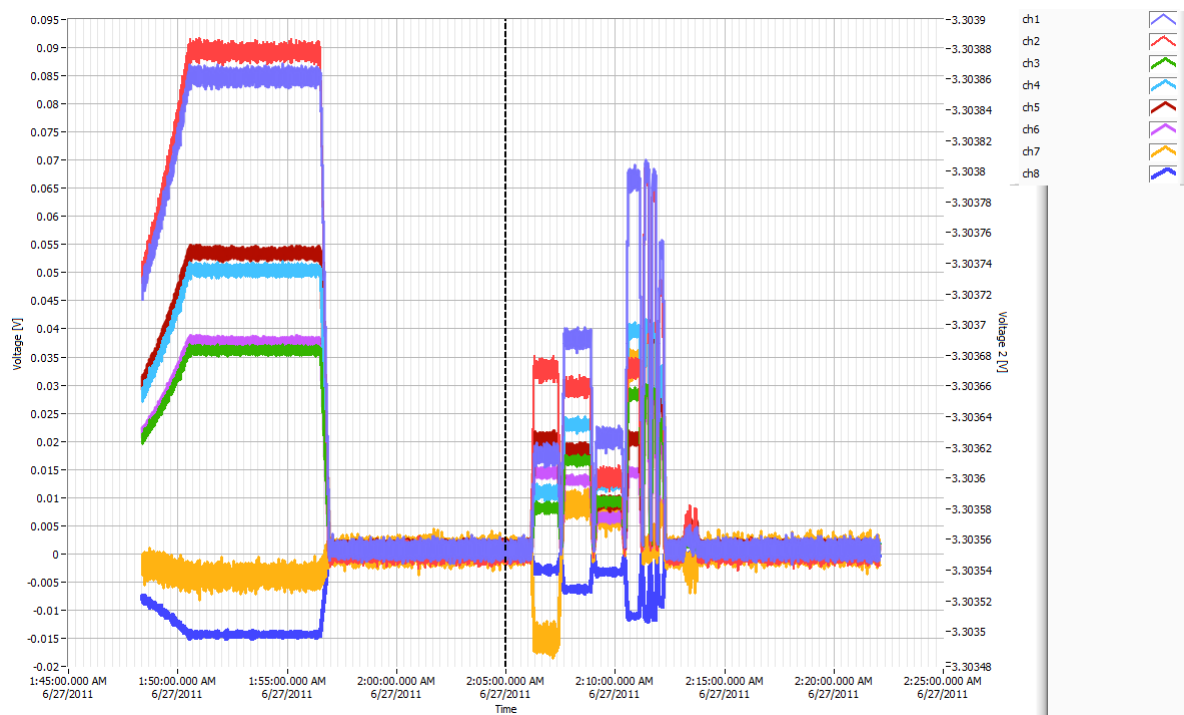


**Figure 10**  
Q6.L8 signals recorded during the current ramp.

Electrical signals (Fig. 11) corresponding to each event of high losses were measured. The shape remained invariable along the series of events, but the size was changing (Fig. 12). It is not yet understood where the signal tail comes from. Even though, a correlation was found between the peak size, the tail size and the tail length (Fig. 13), which allows using only the peak size value for the further analysis.

It is worth mentioning that the peak is very short (less than 100μs) and the acquisition system registered it only as one point. Its nature is not yet fully known.

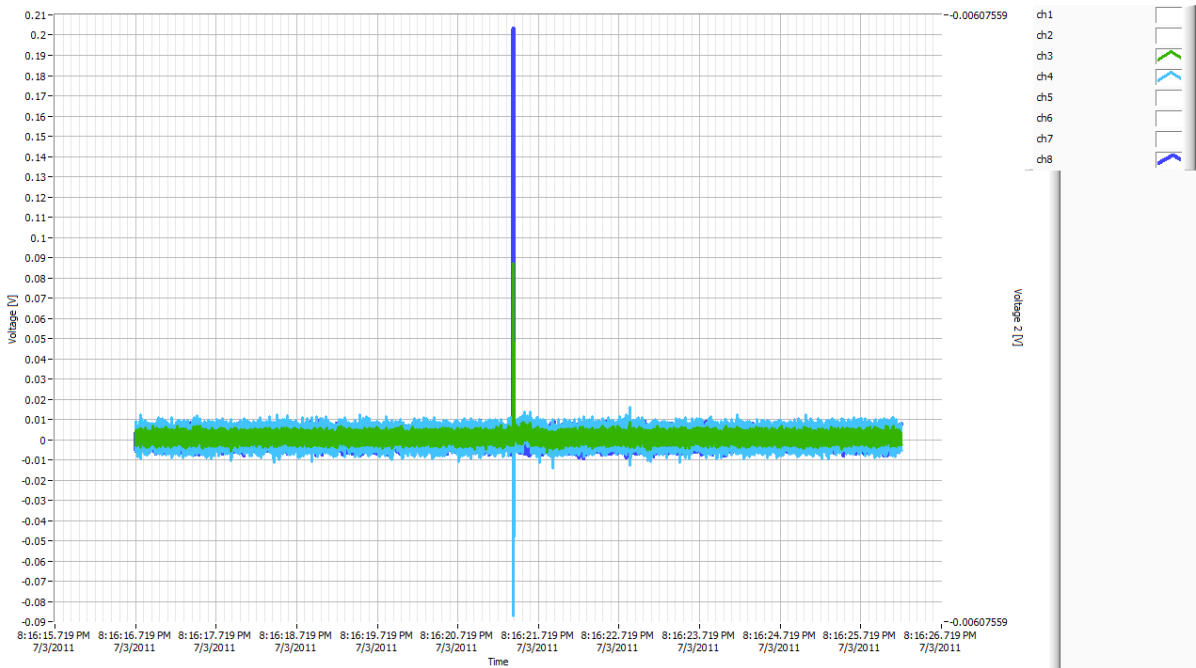


Figure 11.

One of many electrical signals observed on Q6.L8 magnet coil.

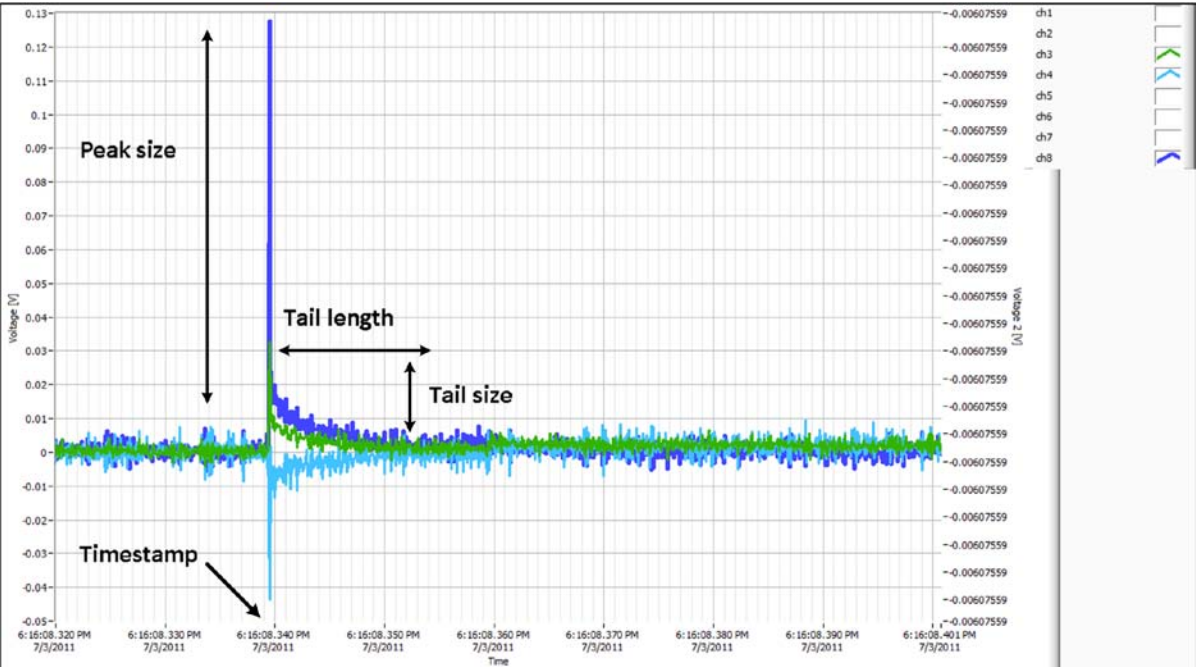
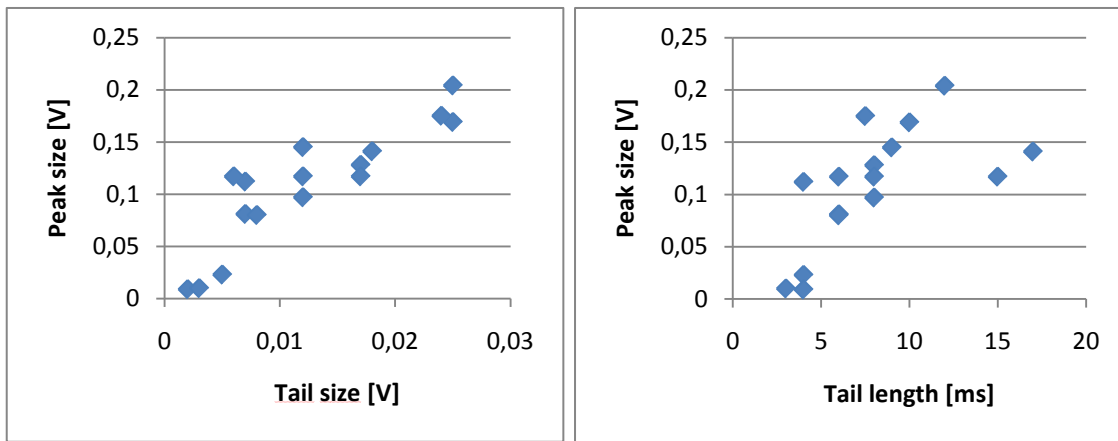


Figure 12

Signal shape.



**Figure 13**

Correlation between the peak size and signal tail parameters.

One can notice that the two channels hooked to the coils constituting the aperture are of an opposite sign. This phenomenon is easy to explain. The power converter is not a current source at the frequency above 100 Hz. It has to be considered as a DC voltage source. A resistive zone showing up in the magnet due to the beam losses will get a resistive voltage drop across. The same voltage drop, but of an opposite sign will be introduced by both coils in the circuit, as the  $dI/dt$  is not 0 anymore (Fig. 14). After a simple calculation one easily come to the conclusion that  $CH3 = -CH4$ .

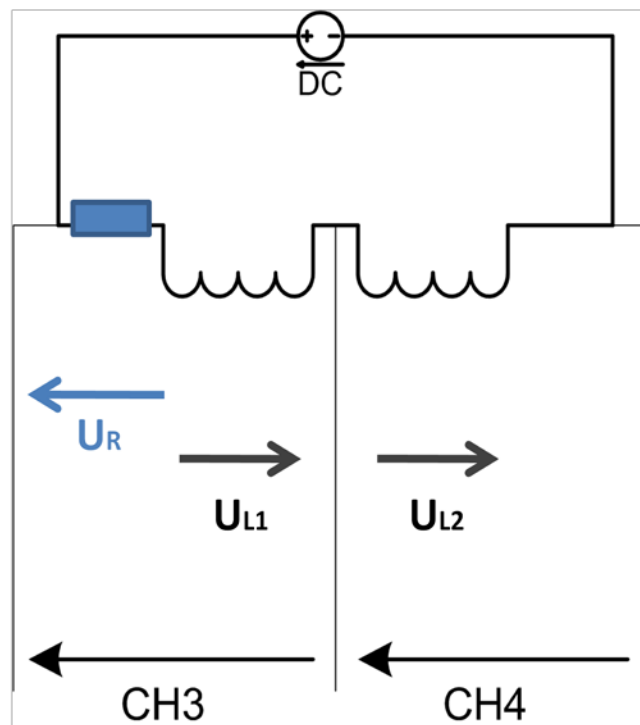


**Figure 14**

Simplified circuit drawing with the voltage drops marked.

In this measurement the DCCT readout of the power converter was not recorded. Even though, it is possible to deduce a small  $di/dt$  at the moment of beam losses. In Fig. 15 the same data set as on Fig. 11 is shown, but each 10 samples is averaged together to get one new point. In this way the noise level is reduced and small (but lower frequency) voltage changes start to be visible. In this case the power converter regulation shows up. After the event of the beam losses a reaction of the PC is visible. It acts against the negative  $di/dt$  originating from the resistive zone in the magnet's coil.

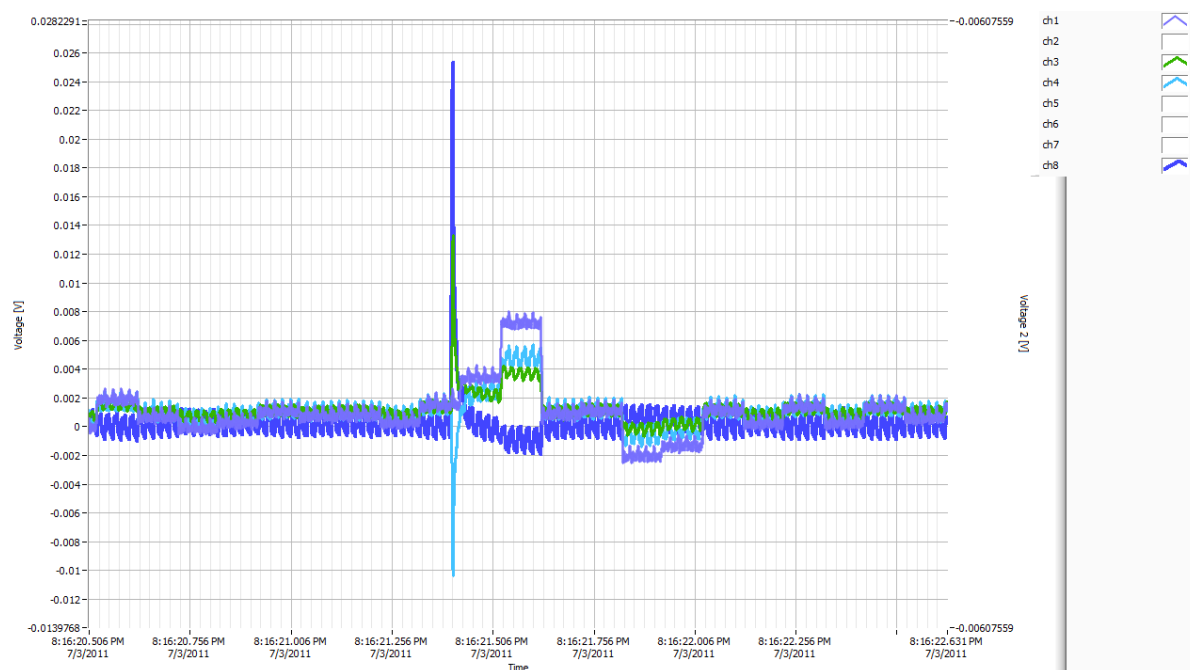


**Figure 15**

Power converter reaction after an event of beam losses.

It has to be noted that the real quench margin will be a function of the current in the magnet. All the measurements mentioned above were done at the current of 176 A, which has to be considered very low for this type of magnet. A precise simulation is not easy. The current dependence should be experimentally confirmed.

### 2.1.3 Correlation between QPS Signal and BLM signal

A correlation between QPS signal and the number of protons lost at the Q6.L8 has been investigated and is presented in Fig. 16. As a first approximation, the QPS signal can be considered proportional to the number of lost protons. The QPS showed a maximum signal of 200 mV, corresponding to  $4.3 \times 10^9$   $p^+$ , but no quench was induced. During the MKI flashover, on April 18<sup>th</sup>, the Q6.L8 quenched and it was estimated that  $4 \times 10^{10}$   $p^+$  were lost at this magnet. The quench limit is then expected to sit in between these two values.

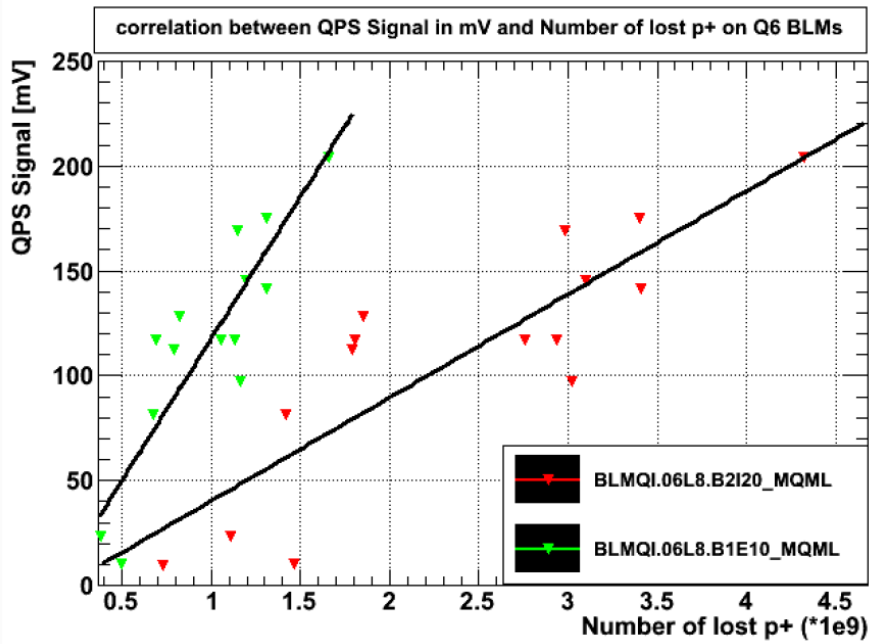


Figure 16

Correlation between the QPS signal and the number of protons lost on Q6.L8. In case B2I20 was saturated the loss was calculated from B1E10 signal by using the ratio factor.

## 2.2 Second method: injection with horizontal bump at Q6.L8

Injection of a low intensity pilot bunch ( $2 \times 10^9$  p<sup>+</sup>) was performed while applying a local orbit bump at the Q6.L8 (see Fig.9). The amplitude of the bump was increased until losses at Q6.L8 induced a dump of the circulating pilot; this amplitude was used for the first injection.

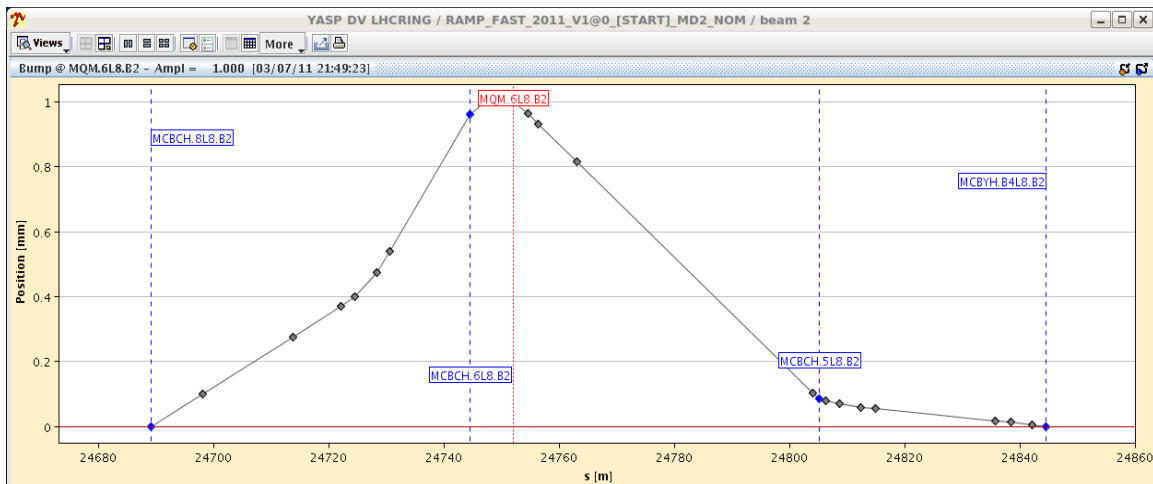


Figure 17

Local orbit bump applied at the location of Q6.L8 in order to try to induce a quench during injection of a low intensity pilot.

The TCLIB was retracted to parking position, while the primary collimators in point 7 staid closed to stop any residual beam.

### 2.2.1 BLM analysis

Three injections, with increasing bump amplitude, were performed and results of the BLM data analysis, at the Q6.L8 magnet, is summarized in Table 3. For all the cases, losses were above the dump threshold which is set up to one third of the quench level. Instead, no signal was recorded by the QPS . This could imply that the estimated quench limit at this magnet could be higher than predictions by a factor of 3.

**Table 3**

Summary of losses recorded at the Q6.L8 and ratio to the dump threshold, for injection with increasing bump amplitude. The BLM was in saturation for the 23 mm bump.

<b>Bump Amplitude [mm]</b>	<b>BLMQI_06L8.B2I20_MQML [Gy/s]</b>	<b>Ratio to dump threshold</b>
21	6.27	3
23	23.60	10
25	21.03	9

No increase of Q6.L8 BLM thresholds have been planned, at present, since losses at this location never showed to be a limitation during injection.

### 2.2.2 QPS analysis

The measurement system installed on the magnet did not capture any signal from the bump. Possibly the loss distribution was such that the magnet coil was not heated up to the normal conducting state. It is also possible that the resistive zones appearing in the magnet were symmetric in both observed coils and the resulting signal was cancelled below the noise level.

## 3. Quench margin for Q4.L6

The quench margin at injection energy was also investigated for the Q4.L6 magnet which is located right downstream of the extraction protection collimators (TCDQ and TCSG). Same technique as the one described in section 2.1 for Q6.L8 was used. In this case, the TCSG collimator in point 6 was closed to  $1.7 \sigma$  gap plus a  $2 \sigma$  offset and the Beam 2 primary collimator in point 3 was used to stop any residual beam (left jaw at -4.5 mm, right jaw at -5.5 mm). Few shots with different intensities were taken: high intensity (up to  $2 \times 10^{10} p^+$ ) was used to determine the quench margin while low intensity ( $5 \times 10^9 p^+$ ) was employed for BLM calibration.

### 3.1.1 BLM analysis

The ionization chambers for B2 at the location of Q4.L6 were in saturation for all the shots corresponding to more than  $1 \times 10^{10} p^+$  injection. The signal for the saturated monitor

BLMQI.04L6.B2I20\_MQY was reconstructed, as in the case of the Q6.L8 BLM, starting from the losses recorded at BLMQI.04L6.B2I20\_MQY (in this case a ratio B2/B1 of 2.7 was found). Results of the BLM data analysis, at the Q4.L6 magnet, show losses of up to a factor ~20 above the dump thresholds while no signal was detected by the QPS. Also in this case thresholds might be too conservative but no action has been taken to increase them.

### 3.1.2 QPS analysis

From the electrical point of view the Q4.L6 magnet is very difficult to measure. All the observed signals were dominated by electromagnetic coupling (Fig. 18) from the dump kickers located physically very close to the DVM system and Q4.L6 magnet.

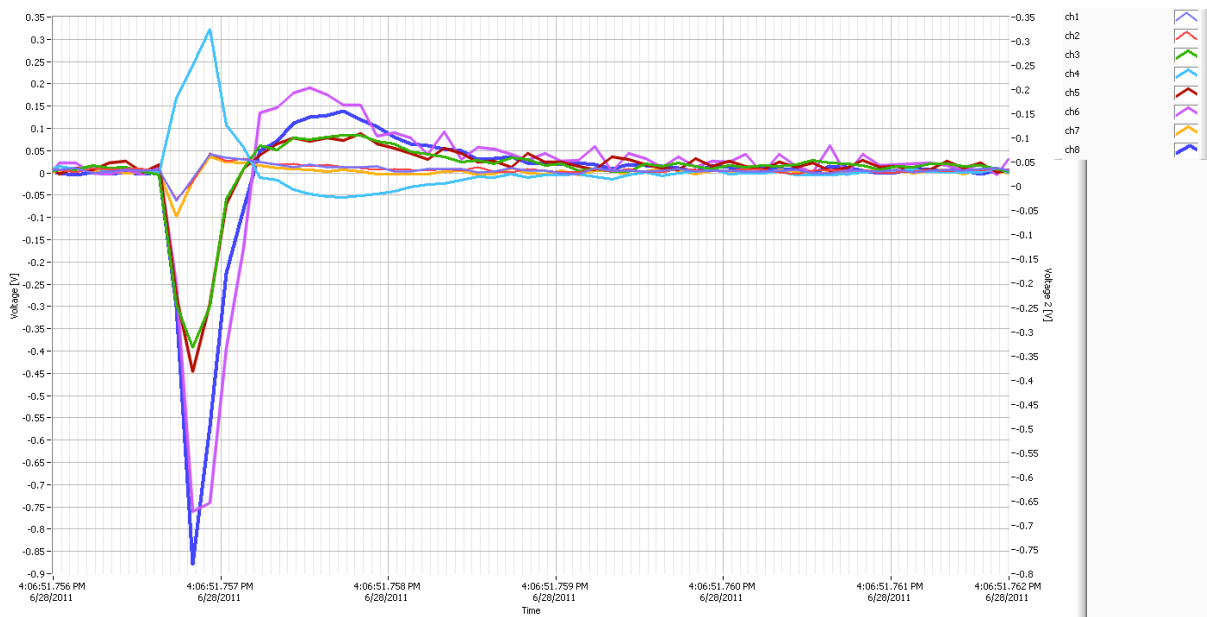


**Figure 18**

Signal seen on Q4.L6 is coming mostly from the electromagnetic coupling with the dump kickers.

The same signal was recorded when the full intensity 3.5 TeV and a pilot 3.5 TeV beams were dumped. It proves that the signal from the beam is too small to be measured.

Knowing that there is one set of kickers per beam and that the measurements were taken only using beam 2, the B1 kickers were disabled to limit the electromagnetic coupling. A new promising signal was recorded (Fig. 19 and Fig. 20). It had a different shape than the signal of Q6.L8. All the channels saw a voltage transient. It seems that this signal comes still from the electromagnetic coupling, but this time from the B2 kickers located about 200 m from Q4.L6. Those can't be disabled for security reasons. Measurement on this magnet cannot be concluded in the current configuration.

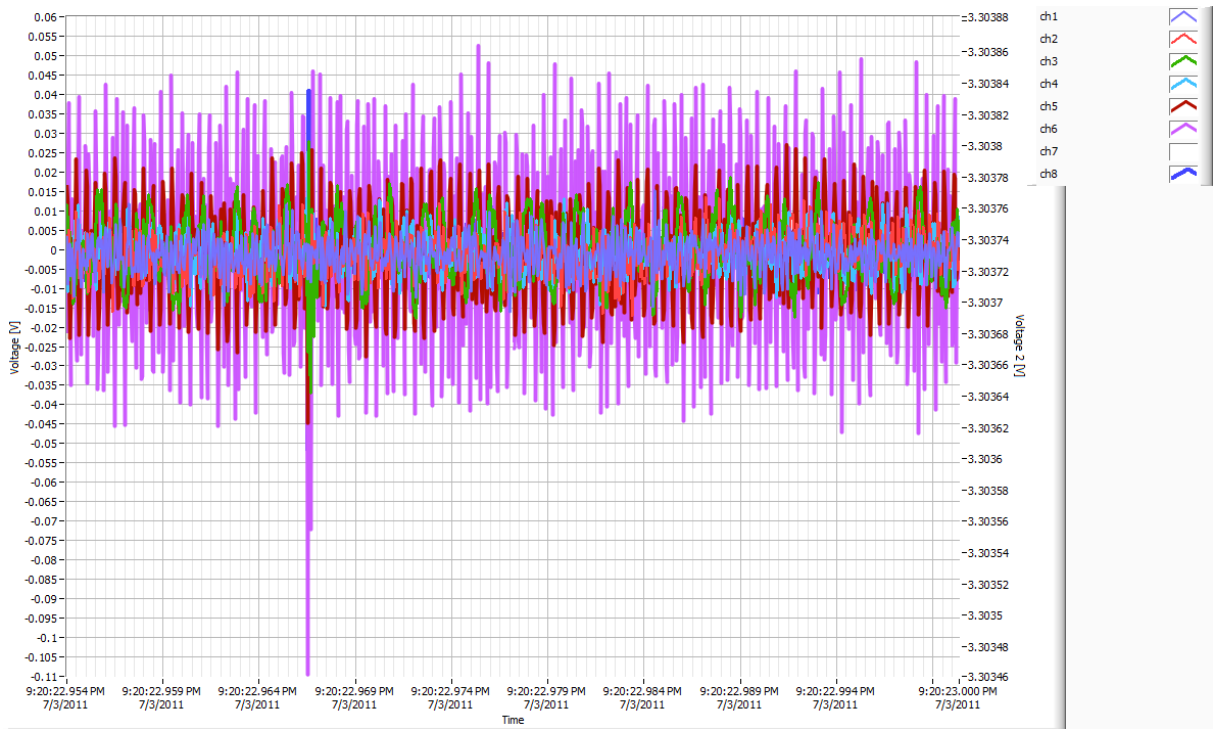


**Figure 19**

Signal from Q4.L6 with B1 kickers disabled.

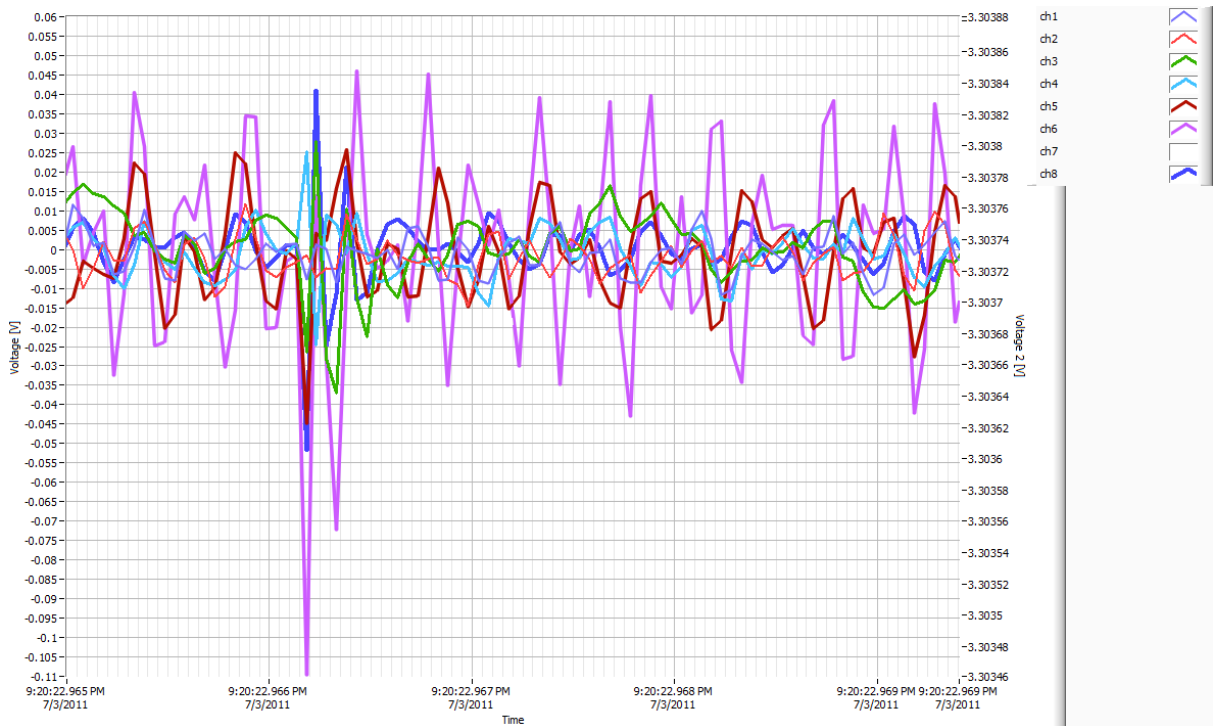


**Figure 20**

Signal from Q4.L6 with B1 kickers disabled, zoomed timescale.



#### 4. Calibration of the Direct Dump BLM.

In this section we discuss the results of the experiment performed in order to calibrate one of the Direct Dump BLMs. This particular Ionization Chamber (IC) is located  $\sim 1$  m downstream of the TCSG.4L6.B2 collimator. On the same support holding the Direct Dump BLM (see Fig. 21) there are three other detectors: two ICs, one of them equipped with an 11 ms filter in order to avoid saturation of the electronics, and one Secondary Emission Monitor (SEM). The first IC, situated about 5 cm above the beam line, continuously saturated the electronics during this exercise and the SEM monitor did not record any signals so these two detectors are not considered in the following analysis. In the following we will refer to the direct dump monitor as BLMDD and to the IC with a filter as BLMEI



**Figure 21**

Views of the location of the different detectors with respect to the secondary collimator (left) and of the position of the three ionization chambers with respect to the beam line.

Eight shots on the TCSG.4L.B2 were provided with intensities ranging from  $0.4E10$  to  $1.6E10$  protons. Table 4 shows a summary of the measurements. The signals observed in BLMEI are presented as dose in the 1.3 s integration window. The BLMDD measurements are presented in ADC counts (BITS) as read out from the electronics. The signals observed in both monitors are normalized to the intensity in order to obtain a calibration factor. Both the signal (right) and the normalized signal (left) are represented versus intensity in Fig. 22 for BLMEI and in Fig. 23 for BLMDD.

Both detectors show approximately linear response with intensity. The large offsets obtained in both linear fits are not compatible with the BLM monitors noise level and they are attributed to saturation in the chambers due to space charge effects. The effect becomes evident as the normalized signal decreases with intensity. The discrepancies in the range of variation of the normalized signals, 35 % for BLMEI and 15 % for BLMDD, are attributed to the relative position of the two detectors with respect to the beam line. Being BLMDD farther away from the center of the shower (beam line), it will receive a lower dose and therefore less affected by space charge. The Calibration Factors, computed as the average of the 8 measurements, are  $(8.63 \pm 1.43) \times 10^{-12}$  (Gy/p) for BLMEI and  $(2.20 \pm 0.17) \times 10^{-6}$  (BITS/p). The errors represent the standard deviation obtained from the 8 measurements.

**Table 4**

Summary of the measurements performed to calibrate the Direct Dump BLM.

Intensity ( $10^{10}$ p)	Signal DD (BITS)	Signal/p ( $10^{-6}$ BITS/p)	Dose BLM (Gy)	Dose/p ( $10^{-12}$ Gy/p)
1.08	24601	2.27	0.0884	8.16
0.75	18151	2.42	0.0728	9.71
1.12	26417	2.35	0.0962	8.59
1.05	21865	2.1	0.0845	8.08
0.38	8893	2.33	0.0429	11.2
0.44	10152	2.3	0.0481	10.9
1.6	31095	1.94	0.1157	7.21
1.55	30256	1.95	0.1131	7.29

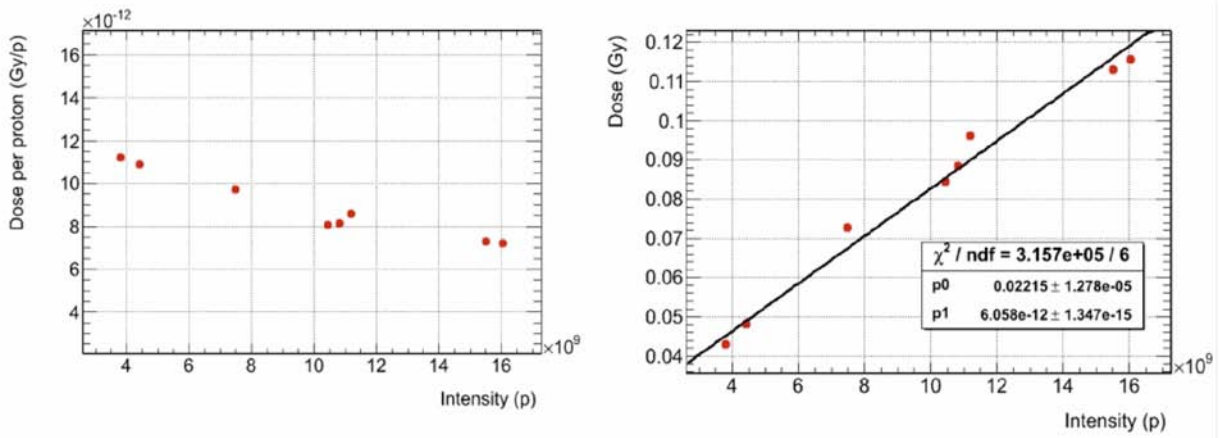


**Figure 22**

Dependence with intensity of the signal and normalized signal observed in BLMEI.

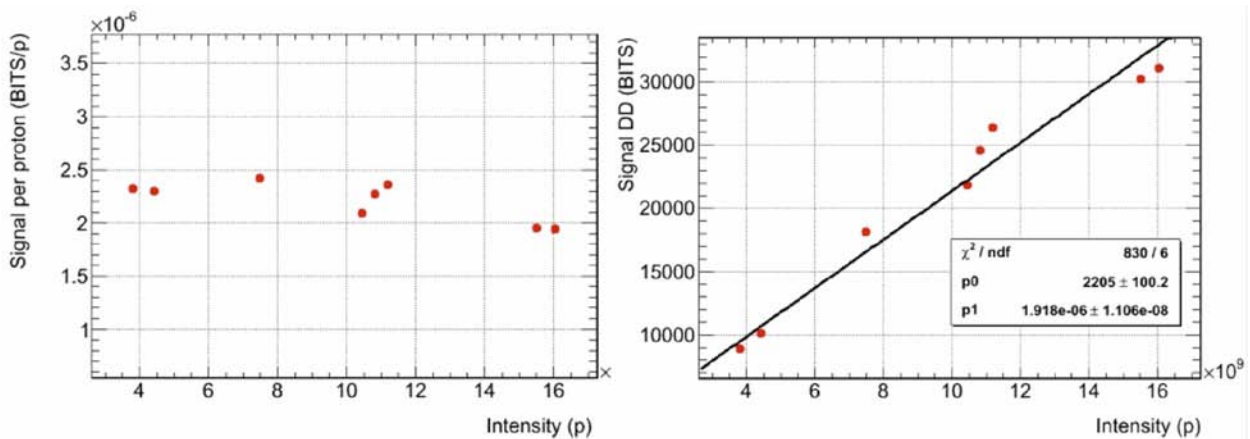


**Figure 23**

Dependence with intensity of the signal and normalized signal observed in BLMDD.

## 5. Conclusions

The results of quench limit investigations for Q6.L8 and Q4.L6 magnets at injection have been presented.

Low intensity beams (from 5E9 to 3E10) have been shot on the TCLIB and TCSG.P6 collimators and the correlation between the signal read on the QPS instrumentation and the losses recorded by the BLM system has been analysed. Although losses well above the estimated quench limit were read at the BLMs, the magnets did not quench and the QPS did not trigger, probably due to the low current at which these magnets are operated at injection (~160 -170 A). No signal on the QPS system was observed also when driving the beam directly into the Q6.L8 magnet with a closed orbit bump.

To further investigate quench margin of Q6.L8, a test will be performed, during the next MD, with a fixed TCLIB configuration, different beam intensities and varying the current in the magnet till the commissioned value (2300 A).

## References

- [1] ATS/Note/2011/040(MD), TI8 Shielding Studies and Angular Alignment of TDI and TCDQ
- [2] MD2-2011: 450 GeV Quench Margin at Injection, EDMS ID: 1149841